Clinical and CT Imaging Differences Between Gastric Schwannoma and Gastric Leiomyoma

Luping Zhao[1], Hongfeng Xue[2], Zhanguo Sun[1], Yueqin Chen[1], Hao Yu[1] and Sen Mao[3]

[1]*Department of Medical Imaging, the Affiliated Hospital of Jining Medical University, Jining, Shandong, China*
[2]*Department of Nutrition, the Affiliated Hospital of Jining Medical University, Jining, Shandong, China*
[3]*Department of Ultrasound, the Affiliated Hospital of Jining Medical University, Jining, Shandong, China*

ABSTRACT

Objective: To determine whether computed tomography (CT) imaging features can be used to differentiate gastric schwannoma (GS) from gastric leiomyoma (GL) and to develop a nomogram as a predictive model.

Study Design: Retrospective study.

Place and Duration of the Study: Department of Medical Imaging, Affiliated Hospital of Jining Medical University, Jining, Shandong, China, from July 2009 to June 2022.

Methodology: Clinical and imaging data of 43 patients with GS and 57 patients with GL were analysed retrospectively. The independent factors for differentiating GS and GL were obtained by the logistic regression analysis. Receiver operating characteristic curve (ROC) was plotted, area under curve (AUC) and calibration tests were used to evaluate the diagnostic efficiency of the model.

Results: The GS group had more females and was older than the GL group ($p < 0.05$). There were statistical differences between the two groups in tumour location, growth mode, LD/SD ratio, necrosis, ulcers, the presence of tumour-associated lymph nodes, enhancement degree, and the HU (Hounsfield units) values of tumour in the venous phase and delayed phase ($p < 0.05$). Logistic regression analysis showed that tumour location, growth mode, LD/SD (long and short diameters) ratio, and the presence of tumour-associated lymph nodes were independent factors in differentiating GS from GL, and a nomogram model was established accordingly. When the model threshold was >0.319, the AUC was 0.987 (95% confidence interval [CI] 0.941~0.999). The sensitivity and specificity were 97.7% and 94.7%, respectively.

Conclusion: The proposed nomogram model based on CT imaging features can be used to differentiate GS from GL.

Key Words: *Gastric leiomyoma, Gastric schwannoma, Computed tomography, Diagnosis.*

How to cite this article: Zhao L, Xue H, Sun Z, Chen Y, Yu H, Mao S. Clinical and CT Imaging Differences Between Gastric Schwannoma and Gastric Leiomyoma. *J Coll Physicians Surg Pak* 2023; **33(04)**:369-373.

INTRODUCTION

Gastrointestinal stromal tumours (GISTs), neurogenic tumours, and myogenic tumours are three major categories of gastric submucosal tumours (SMTs). The most representative types of neurogenic and myogenic tumours are gastric schwannoma (GS) and gastric leiomyoma (GL), respectively.[1] With the development of medical technology, endoscopic ultrasound (US), magnetic resonance imaging (MRI), and computed tomography (CT) have been used for the detection of gastric diseases. Although endoscopic US has demonstrated the diagnostic value for the accurate characterisation of gastric lesions, it is invasive and dependent on operator skill.[2] MRI is a time-consuming methodology easily leading to motion artefacts, which limits its application in the detection of gastrointestinal diseases.[3] Therefore, CT as a non-invasive and economical imaging method is used to differentiate them.[4] The most common gastric SMT is GIST, and many studies had shown that CT had high diagnostic value in differentiating GS and GIST, as well as GL and GIST.[5,6] However, there were few reports on the CT differential diagnosis of GS and GL.

At present, as a statistical model for the individualised prediction and analysis of clinical events, nomograms had been widely used in the differential diagnosis and risk prediction of various diseases.[7,8] Therefore, this research intended to retrospectively analyse the CT imaging features of GS and GL, to develop a nomogram model based on the results of logistic regression analysis to explore the diagnostic value of CT in differentiating GS and GL to further improve the ability to preoperatively diagnose them. The objective of this study was to determine whether computed tomography (CT) imaging features can be used to differentiate gastric schwannoma (GS) from gastric leiomyoma (GL) and to develop a nomogram as a predictive model.

Correspondence to: Dr. Sen Mao, Department of Ultrasound, Affiliated Hospital of Jining Medical University, Jining, Shandong, China
E-mail: xiaomao_s@sina.com

Received: November 04, 2022; Revised: February 09, 2023; Accepted: March 31, 2023
DOI: https://doi.org/10.29271/jcpsp.2023.04.369

METHODOLOGY

The clinical and CT imaging data of 43 patients with GS and 57 patients with GL proved by histopathology after surgery were analysed retrospectively. The inclusion criteria were a diagnosis of GS or GL by postoperative histopathology; plain and enhanced CT scans of the upper abdomen performed before surgery; and lesion size over 1cm in diameter. The exclusion criteria were the concomitant presence of other tumours and the unavailability of the CT images.

A Siemens Somatom definition or definition flash spiral CT scanner was used. All 100 patients underwent the abdominal CT examination. Three minutes prior to scanning, 500-1000 mL of warm water was drunk to fill the stomach cavity. The CT parameters were as follows: Tube voltage of 120 KV, tube current of 230 mA, matrix 512×512, pitch of 1.0, and reconstruction layer thickness of 1.0 mm. Eighty millilitres of nonionic iodinated contrast material (350 mg I/mL or 370 mg I/mL) was injected through the anterior elbow vein using a double-barbed high-pressure syringe at a flow rate of 3.0-3.5 mL/s. Arterial, venous, and delayed phase scans were obtained at 25~30 s, 60~65 s, and 120~140 s after contrast injection, respectively.

Two radiologists in abdominal CT diagnosis reviewed the images independently, and the final results were obtained through the consultation in case of disagreement. Tumour location was described as the upper, middle, or lower parts of the stomach.[9] Growth mode was described as intraluminal type, extraluminal type or mixed type. Shape was described as regular or irregular; long diameter (LD) and short diameter (SD) ratio of the central slice of each mass were the maximum and minimum measurements in cm and then the LD/SD ratio was calculated.[10] The HU mean value of the measurements taken, at the maximum cross-sectional central location of the tumour was noted. A higher CT value of tumour in the venous phase or delayed phase minus non-enhanced phase, by <20 HU, 20-40 HU and >40 HU indicated mild, moderate, and significant enhancement, respectively.[10] Presence or absence or necrosis, calcification, or ulceration was noted.[8] Tumour-associated lymph nodes around the tumour were evaluated as inflammatory reactive hyperplasia or metastatic by pathology and their subsequent size reduction after postoperative follow-up was recorded as present or absent.

Statistical tests were performed using the Statistical Package for Social Sciences software version 26.0 (IBM, Chicago, IL, USA), MedCalc15.2.2, and R software (version 4.1.3; http://www.R-project.org). The conformity of the variables to the normal distribution was examined using Shapiro Wilk tests. Normally distributed continuous variables were given as mean and standard deviation (SD), while non-normally distributed variables were given as median (Q1-Q3), independent samples t-test was used to compare the two groups with normal distribution; otherwise, the Mann–Whitney U test was used. Qualitative data were shown as frequencies (percentages). Chi-square tests were applied for categorical variables. Each variable that was statistically significant in univariate analysis was subjected to the logistic regression analysis to confirm independent influencing factors in differentiating GS and GL and then a nomogram was constructed. Calibration was evaluated by the Hosmer–Lemeshow goodness-of-fit test and the area under curve (AUC) were used to evaluate the diagnostic efficiency of the model. The value of $p < 0.05$ was considered statistically significant.

RESULTS

The proportion of female patients in the GS group was significantly higher than that in the GL group, and the average age of patients in the GS group was slightly older than that in the GL group ($p < 0.05$). The clinical symptoms of patients in both groups mainly included abdominal pain and discomfort, rarer symptoms included melena and haematemesis, asymptomatic patients were mostly identified during physical examination, and there was no significant difference between the two groups ($p > 0.05$, Table I).

Table I: Clinical characteristics and CT imaging features.

Clinical Characteristics/ CT Imaging Features	GS (n=43)	GL (n=57)	p-value
Age, Mean ±SD	58.47±10.49	51.16±9.69	<0.001[a]
Sex			0.004[b]
Male	6 (13.95%)	23 (40.35%)	
Female	37 (86.05%)	34 (59.65%)	
Clinical Symptoms			0.111[b]
Yes	28 (65.12%)	28 (49.12%)	
No	15 (34.88%)	29 (50.88%)	
Location			<0.001[b]
Upper Stomach	6 (13.95%)	40 (70.18%)	
Central Stomach	29 (67.44%)	15 (26.32%)	
Lower Stomach	8 (18.61%)	2 (3.5%)	
Shape			0.086[b]
Regular	34 (79.07%)	36 (63.16%)	
Irregular	9 (20.93%)	21 (36.84%)	
Growth Mode			<0.001[b]
Intraluminal Type	8 (18.60%)	53 (92.98%)	
Extraluminal or Mixed Type	35 (81.40%)	4 (7.02%)	
LD/SD Ratio, Median (Q1-Q3)	1.23 (1.12-1.43)	1.69 (1.40-2.04)	<0.001[c]
Necrosis			<0.001[b]
Yes	13 (30.23%)	1 (1.75%)	
No	30 (69.77%)	56 (98.25%)	
Calcification			0.253[b]
Yes	7 (16.28%)	5 (8.77%)	
No	36 (83.72%)	52 (91.23%)	
Ulcer			0.008[b]
Yes	10 (23.26%)	3 (5.26%)	
No	33 (76.74%)	54 (94.74%)	
Tumour-Associated Lymph Node			<0.001[b]
Yes	27 (62.79%)	2 (3.51%)	
No	16 (37.21%)	55 (96.49%)	
Enhancement Degree			<0.001[b]
Mild to Moderate Enhancement	21 (48.84%)	54 (94.74%)	
Significant Enhancement	22 (51.16%)	3 (5.26%)	
CT Value (HU)			
Non-enhanced Phase, Mean ±SD	36.79±3.73	37.53±4.83	0.409[a]
Arterial Phase, Median (Q1-Q3)	47 (44-59)	49 (45-52)	0.856[c]
Venous Phase, Median (Q1-Q3)	67 (59-73)	58 (52-64)	<0.001[c]
Delay Phase, Median (Q1-Q3)	78 (69-87)	63 (59-70)	<0.001[c]

[a] *Independent t-test was used;* [b] *Chi-Square test was used;* [c] *Mann Whitney U-test was used.*

In the GS group, most of the tumours were in the central and lower parts of the stomach, with a regular shape such as round or oval, and mainly extraluminal or mixed growth. Lymph nodes of varying sizes were common around the tumour. In the GL group, most of the tumours were found in the upper part of the stomach, about half of which were irregular in shape, and mainly of intraluminal growth. The LD/SD ratio of the GS group

was significantly lower than that of the GL group. Necrosis, ulcer, and calcification were rare in both groups, but the incidence of necrosis and ulcer in the GS group was higher than that in the GL group. In the GS group, multiple lymph nodes of different sizes were common around the tumour, of which 11 cases were surgically resected and pathologically confirmed with inflammatory reactive hyperplasia. The peritumoural lymph nodes of the other 16 cases were not removed due to the limitation of surgical methods, but all of them became smaller or disappeared after postoperative follow-up. In the GL group, only two cases had peritumoural lymph nodes, which were proved to be inflammatory reactive hyperplasia by surgery and pathology. Approximately half of tumours in GS group showed significant enhancement, while most of tumours in the GL group showed mild to moderate enhancement, and the CT values of tumours in the GS group were significantly higher than those in the GL group in the venous phase and delay phase (Table I).

Logistic regression analysis showed that tumour location, growth mode, LD/SD ratio, and the presence of tumour-associated lymph nodes were independent influencing factors in differentiating GS and GL. The optimal threshold of the LD/SD ratio for a diagnosis of GS was ≤1.32 (Table II). A nomogram model was subsequently established (Figure 1).

Table II: Logistic regression analysis for GS diagnosis predictors.

Constants and Variables	Co-efficient	Cut-off Value	Odds ratio (95% CI)	P
Constant	4.839			0.083
Location (Central or Lower Stomach)	2.464	-	11.755 (1.431~96.546)	0.022
Growth Mode (Extraluminal or Mixed Type)	4.373	-	79.307 (6.197~1014.928)	0.001
Tumour-Associated Lymph Node (Present)	3.037	-	20.841 (1.177~369.188)	0.038
LD/SD Ratio	-6.198	≤1.32	0.002 (0~0.132)	0.004

The results of the Hosmer-Lemeshow goodness-of-fit test (χ^2=8.6422; p=0.373) indicated that predictive model had great calibration. When the model threshold was >0.319, the AUC value was 0.987 (95% CI 0.941-0.999), and the sensitivity and specificity were 97.7% and 94.7%, respectively.

DISCUSSION

The age, gender, tumour location, growth mode, LD/SD ratio, necrosis, ulcers, the presence of tumour-associated lymph nodes, enhancement degree, and CT values of tumour in the venous phase and delayed phase were all conducive to differentiate GS from GL in this study. Tumour location, growth mode, LD/SD ratio, and the presence of tumour-associated lymph nodes could be used as independent influencing factors for the differential diagnosis of the two tumours. The nomogram model based on the results of logistic regression analysis had higher diagnostic efficiency, sensitivity, and specificity, and the calibration curve showed that the probability of GS predicted by the nomogram was in good agreement with the actual value. The model provided a relatively reliable and intuitive method for the preoperative differentiation of GS and GL.

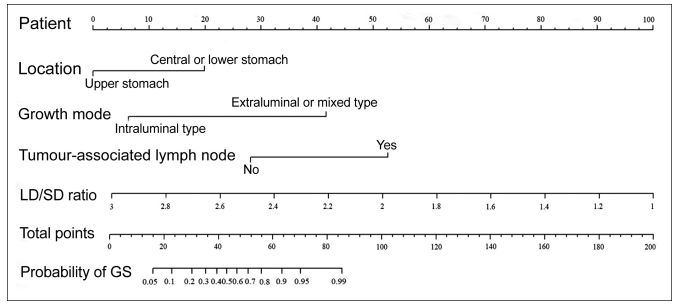

Figure 1: Nomogram built from independent influencing factors: Tumour location, growth mode, LD/SD ratio, and presence of tumour-associated lymph nodes.

In this study, GS mostly occurred in the central and lower parts of the stomach (37/43, 86.05%), typically with extravascular or mixed growth (35/43, 81.40%), which is consistent with previous reports.[11-15] GL mainly occurred in the upper stomach (40/57, 70.18%), with intraluminal growth (53/57, 92.98%), which is also consistent with previous reports.[6,10,16,17] However, the proportion of intraluminal growth was higher among GL in this study. It may be related to the location of the tumour and the growth mode of the tumour is more likely to show clinical symptoms or be detected on gastroscopy. Since GL originates from the cardia of the stomach,[18] morphological diversity easily develops due to the restriction of the gastric wall muscle layer and cardiac sphincter during the growth process, which makes the tumour grow along the stomach wall. Although GS was more likely to occur in the body of the stomach, the growth of the resistance of the tumour in all directions was relatively small, and the tumour demonstrated a regular shape, mostly round or oval. Therefore, the LD/SD ratio of GS was usually less than that of GL. The results of this study showed that the LD/SD ratio ≤1.32 was the best threshold, which was close to previous literature with the LD/SD ratio <1.2.[17]

In this study, there was a significant difference in the presence of tumour-associated lymph nodes between the two groups. Peritumoural lymph nodes around GS were common (27/43, 62.79%), multiple and varied in size, mostly round and oval in shape but some showing irregular shapes, and the short diameters of most lymph nodes were less than 1 cm. Peritumoural lymph nodes around GL were rare, seen in only two patients in this study, and the short diameter of the lymph nodes was less than 1 cm. The number of peritumoural lymph nodes around GS was higher than that around GL, which may be related to the lymphocyte sheath around the tumour, which was a typical histopathological manifestation of GS. Some studies stated that the peritumoural lymph nodes around GS were mostly inflammatory reactive hyperplastic and swollen lymph nodes[6,13,15,17,19,20]; the present authors agree with this view. In this study, 13 cases (2 with GL and 11 with GS) with peritumoural lymph nodes underwent surgical resection, and pathology confirmed the presence of inflammatory reactive hyperplasia; for the other 16 cases, the peritumoural lymph nodes became smaller or disappeared after postoperative follow-up observation, suggesting that it was related to reac-

tive hyperplasia in peritumoural lymph nodes stimulated by cytokines generated by GS peritumoural lymphocytes.

This study has some shortcomings. Firstly, due to the large time span over which the patients were enrolled, differences in the types of contrast agents and CT models used may lead to deviations in the measurement indexes. Secondly, due to the small number of tumours with specific sites and growth modes, the combined classifications may have a certain influence on the results. Thirdly, the sample was small in number and came from a single centre; as this study lacked external validation, so the results are not sufficiently robust.

CONCLUSION

The nomogram model based on tumour location, growth mode, LD/SD ratio, and the presence of tumour-associated lymph nodes could be used to distinguish GS from GL. For radiologists and clinicians, it is a convenient, intuitive, and relatively reliable model. Prospective studies with larger sample sizes are needed to validate and improve the model in the future.

FUNDING:
2022 Jining key research and development plan project (2022YXNS033); 2021 Jining key research and development plan project (2021YXNS020).

ETHICAL APPROVAL:
This retrospective study was approved by the institutional review board of the Affiliated Hospital of Jining Medical University (2021C018).

PATIENTS' CONSENT:
Not applicable as the data were obtained retrospectively.

COMPETING INTEREST:
The authors declared no competing interest.

AUTHORS' CONTRIBUTION:
LZ: Conception and design, drafting of the manuscript.
HX, SM: Material preparation and data collection.
HY, SM: Data analysis.
YC, ZS: Guidance and revision of the manuscript.
All the authors have approved the final version of the manuscript to be published.

REFERENCES

1. Chen Z, Yang J, Sun J, Wang P. Gastric gastrointestinal stromal tumours (2-5 cm): Correlation of CT features with malignancy and differential diagnosis. *Eur J Radiol* 2020; **123**:108783. doi: 10.1016/j.ejrad.2019.108783.
2. Kim JY, Lee JM, Kim KW, Park HS, Choi JY, Kim SH, *et al*. Ectopic pancreas: CT findings with emphasis on differentiation from small gastrointestinal stromal tumor and leiomyoma. *Radiol* 2009; **252(1)**:92-100. doi: 10.1148/radiol.2521081441.
3. Kaltenbach B, Roman A, Polkowski C, Gruber-Rouh T, Bauer RW, Hammerstingl R, *et al*. Free-breathing dynamic liver examination using a radial 3D T1-weighted gradient echo sequence with moderate undersampling for patients with limited breath-holding capacity. *Eur J Radiol* 2017; **86**: 26-32. doi: 10.1016/j.ejrad.2016.11.003.
4. Scola D, Bahoura L, Copelan A, Shirkhoda A, Sokhandon F. Getting the GIST: A pictorial review of the various patterns of presentation of gastrointestinal stromal tumors on imaging. *Abdom Radiol (NY)* 2017; **42(5)**:1350-64. doi: 10.1007/s00261-016-1025-z
5. Wang J, Zhou X, Xu F, Ao W, Hu H. Value of CT imaging in the differentiation of gastric leiomyoma from gastric stromal tumor. *Can Assoc Radiol J* 2021; **72(3)**:444-51. doi: 10.1177/0846537119885671.
6. Jin Wook C, Dongil C, Kyoung-Mee K, Sung Sohn T, Haeng Lee J, Jung H, *et al*. Small submucosal tumors of the stomach: Differentiation of gastric schwannoma from gastrointestinal stromal tumor with CT. *Korean J Radiol* 2012, **13(4)**:425-33. http://doi.org/10.3348/kjr.2012.13.4.425.
7. Sun XF, Zhu HT, Ji WY, Zhang XY, Li XT, Tang L, *et al*. Preoperative prediction of malignant potential of 2-5 cm gastric gastrointestinal stromal tumors by computerised tomography-based radiomics. *World J Gastrointest Oncol* 2022; **14(5)**:1014-26. doi: 10.4251/wjgo.v14.i5.1014.
8. Shao C, Feng X, Yu J, Meng Y, Liu F, Zhang H, *et al*. A nomogram for predicting pancreatic mucinous cystic neoplasm and serous cystic neoplasm. *Abdom Radiol (NY)* 2021; **46(8)**:3963-73. doi: 10.1007/s00261-021-03038-3.
9. Japanese gastric cancer association. Japanese classification of gastric carcinoma: 3rd English edition. *Gastric Cancer* 2011; **14(2)**:101-12. doi: 10.1007/s10120-011-0041-5.
10. Jian-Xia X, Qiao-Ling D, Yuan-Fei L. A scoring model for radiologic diagnosis of gastric leiomyomas (GL) with contrast-enhanced computed tomography (CE-CT): Differential diagnosis from gastrointestinal stromal tumors (GISTs). *Eur J Radiol* 2021, **134**:109395. doi: 10.1016/j.ejrad.2020.109395.
11. Wei W, Kaiming C, Yang H. Computed tomographic characteristics of gastric schwannoma. *J Int Med Res* 2019, **47(5)**:1975-86. oi: 10.1177/0300060519833539.
12. Zhong Z, Xu Y, Liu J, Zhang C, Xiao Z, Xia Y, *et al*. Clinicopathological study of gastric schwannoma and review of related literature. *BMC Surg* 2022; **22(1)**:159. doi: 10.1186/s12893-022-01613-z.
13. Wang J, Zhang W, Zhou X, Xu J. Simple analysis of the computed tomography features of gastric schwannoma. *Can Assoc Radiol J* 2019; **70(3)**:246-53. doi: 10.1016/j.carj.2018.09.002.
14. Ji JS, Lu CY, Mao WB, Wang ZF, Xu M. Gastric schwannoma: CT findings and clinicopathologic correlation. *Abdom Imag* 2015; **40(5)**:1164-9. doi: 10.1007/s00261-014-0260-4.
15. Xu JX, Yu JN, Wang XJ, Xiong YX, Lu YF, Zhou JP, *et al*. A radiologic diagnostic scoring model based on CT features for differentiating gastric schwannoma from gastric gastrointestinal stromal tumors. *Am J Cancer Res* 2022; **12(1)**: 303-4.
16. Zhu H, Chen H, Zhang S, Peng W. Differentiation of gastric true leiomyoma from gastric stromal tumor based on biphasic contrast-enhanced computed tomographic findings. *J Comput Assist Tomogr* 2014; **38(2)**:228-34. doi: 10.1097/RCT.0b013e3182ab0934.

17. Hyun Kyung Y, Young Hoon K, Yoon Jin L. Leiomyomas in the gastric cardia: CT findings and differentiation from gastrointestinal stromal tumors. *Eur J Radiol* 2015; **84(9)**: 1694-700.

18. Okanoue S, Iwamuro M, Tanaka T, Satomi T, Hamada K, Sakae H, *et al*. Scoring systems for differentiating gastrointestinal stromal tumors and schwannomas from leiomyomas in the stomach. *Medicine (Baltimore)* 2021; **100(40)**:e27520. doi: 10.1097/MD.0000000000027520.

19. Choi YR, Kim SH, Kim SA, Shin CI, Kim HJ, Kim SH, *et al*. Differentiation of large (≥5 cm) gastrointestinal stromal tumors from benign subepithelial tumors in the stomach: Radiologists' performance using CT. *Eur J Radiol* 2014; **83(2)**:250-60.

20. Liu M, Liu L, Jin E. Gastric sub-epithelial tumors: Identification of gastrointestinal stromal tumors using CT with a practical scoring method. *Gastric Cancer* 2019; **22(4)**:769-77. doi: 10.1007/s10120- 018-00908-6.